Equilibrium Grain Boundary Segregation of Antimony in Iron Base Alloys

Ravnotežna segregacija antimona po mejah zrn v zlitinah železa in antimona

R. Mast[1], H. Viefhaus, M. Lucas, H. J. Grabke, Max-Planck-Institute, Düsseldorf, Germany

Prejem rokopisa - received: 1996-10-01; sprejem za objavo - accepted for publication: 1996-11-04

The equilibrium grain boundary segregation of antimony was investigated in iron base alloys (Fe-Sb, Fe-C-Sb, Fe-Ni-Sb) after annealing at temperatures between 550°C and 750°C. Utilizing Auger electron spectroscopy (AES) the concentration of antimony at intergranular fracture faces was determined as a function of bulk concentration and equilibration temperature. The segregation of antimony in Fe-Sb alloys with 0,012 wt.% - 0,094 wt.% Sb was described by the Langmuir-McLean equation. The evaluation leads to the free enthalpy of segregation $\Delta G_{segr.}$ = -19 kJ/mol - T 28 J/mol K. For Fe-0,93 wt.% Sb and Fe-1,91 wt.% Sb a thermodynamic calculation is not possible because of intergranular antimonides had formed. Scanning electron micrographs (SEM) of fractured samples show that the percentage of intergranular fracture increases with an increasing coverage of antimony at the grain boundaries. The addition of carbon to Fe-Sb alloys results in a higher grain boundary cohesion which is caused by two effects of carbon, displacement of antimony from the grain boundaries by carbon and enhanced grain boundary cohesion. In the Fe-Ni-Sb alloys an additional segregation of nickel was found at the grain boundaries but no enhanced antimony segregation, as expected from previous models of other authors, assuming Ni-Sb cosegregation.

Key words: grain boundary segregation, antimony equilibrium segregation, Fe-Sb alloys, Fe-C-Sb alloys, Fe-Ni-Sb alloys, segregation thermodynamics, Langmuir-McLean equation, Auger electron spectroscopy (AES), intergranular fracture, embrittlement, site competition, Charpy impact tests

Ravnotežna segregacija antimona po mejah zrn v zlitinah z železnoosnovno (Fe-Sb, Fe-C-Sb, Fe-Ni-Sb) po žarjenju v temperaturnem področju od 550°C do 750°C. Z metodo spektroskopije Augerjevih elektronov (AES) je bila določena koncentracija antimona na interkristalnih prelomnih ploskvah kot funkcija vsebnosti antimona v osnovnem materialu in ravnotežne temperature. Segregacija antimona v Fe-Sb zlitinah z 0.012 ut.% - 0,094 ut.% Sb je opisana z Langmuir McLeanovo enačbo izračunana je bila prosta entalpija segregacije $\Delta G_{segr.}$ = -19 kJ/mol - T 28 J/mol K. Za zlitini Fe -0,93 ut.% Sb in Fe -0,91 ut.% Sb termodinamični izračuni niso mogoči zaradi tvorbe interkristalnih antimonidov. Posnetek z vrstičnim elektronskim mikroanalizatorjem (SEM) prelomljenih vzorcev kaže, da odstotek interkristalnega preloma narašča z naraščajočo segregirano plastjo antimona na mejah zrn. Dodatek ogljika v Fe-Sb zlitino povzroči večjo kohezijo med posameznimi zrni, ogljik namreč izrine antimon z mej zrn in zviša kohezijo kristalnih mej. V Fe-Ni-Sb zlitinah je bila določena še segregacija niklja na mejah zrn ne pa tudi povečana koncentracija antimona kot je bilo pričakovati po prejšnjih modelih nekaterih avtorjev, ki so predvideli skupno segregacijo Ni-Sb.

Ključne besede: segregacija na mejah zrn, ravnotežna segregacija antimona, Fe-Sb zlitine, Fe-C-Sb zlitine, Fe-Ni-Sb zlitine, termodinamika segregacij, Langmuir McLeanova enačba, spektroskopija Augerjevih elektronov (AES), interkristalni prelom, krhkost, tekmovanje za prosta mesta na površini, Charpyjev udarni preizkus

1 Introduction

The increased usage of low quality scrap in steel production will lead to a higher content of antimony in steels, which may have a deleterious effect on material properties. The presence of antimony (and/or other tramp elements such as P, Sn, S, As) induces temper embrittlement of low alloy ferritic steels by segregation to the grain boundaries during application at higher temperatures[1,2,3]. The driving forces for such an enrichment in a range of a monolayer are the decrease of interfacial energy and the release of elastic energy. Especially the latter effect is important for antimony because of its large atom size compared to iron atoms. Many researches have been shown that the amount of antimony segregation depends on the total composition of the steel. However, there is no uniform evidence how other alloying components, especially nickel[2,4,5], influence antimony segregation.

Therefore, the equilibrium grain boundary segregation of antimony and its effects on material properties were examined in simple iron base alloys to avoid the complex chemistry of multicomponent steels. The degree of coverage was determined by Auger electron spectroscopy (AES) on the intergranular fracture faces after fracture by impact inside the UHV chamber. The influence on the mechanical behaviour was studied by scanning electron microscopy (SEM) and Charpy impact tests.

2 Experimental procedure

The alloys used in this study were melted in a vacuum induction furnace. The chemical compositions are listed in **Table 1**. Small amounts of manganese (0,02 wt.%) were added to each alloy to tie up sulfur, which has a strong tendency for grain boundary segregation[3] and may hinder antimony segregation.

The ingots of the Fe-Sb, Fe-C-Sb and Fe-Ni-Sb alloys were hot forged and then machined into rectangular specimens. The Fe-Sb and Fe-Ni-Sb samples were heat treated by austenitizing at 1060°C for 70-90 min, air

[1] Dr.Sc. Ralph MAST
Max-Planck-Institut für Eisenforschung GmbH
Postfach 140 444, 40074 Düsseldorf, Germany

Table 1: Chemical composition of the Fe-Sb, Fe-C-Sb and Fe-Ni-Sb alloys (wt.%)

Alloy	Sb	C	Mn	P	S
Fe-Sb1	0,012	0,005	0,027	0,0015	0,0013
Fe-Sb2	0,049	0,0048	0,027	0,0011	0,001
Fe-Sb3	0,094	0,0057	0,027	0,001	0,0011
Fe-Sb4	0,93	0,006	0,026	0,0013	0,0012
Fe-Sb5	1,91	0,0039	0,028	0,0014	0,0012
Fe-C-Sb1	0,056	0,0043	0,025	<0,002	0,0013
Fe-C-Sb2	0,053	0,0085	0,023	<0,002	0,0013
Fe-C-Sb3	0,052	0,0144	0,023	<0,002	0,0014
Fe-C-Sb4	0,094	0,0057	0,027	0,001	0,0011

Alloy	Sb	Ni	C	Mn	P
Fe-Ni-Sb1	0,049	0,53	0,0035	0,022	<0,002
Fe-Ni-Sb2	0,049	2,85	0,0069	0,024	<0,002

cooling, and then tempering at 780°C for 168 h and water quenching. These two heat treatments were performed in flowing wet hydrogen to decrease the bulk carbon concentration below 10 wt.-ppm.

The Fe-C-Sb alloys were annealed in flowing dry argon to avoid carbon losses. The samples were homogenized at 1060°C for 70 min and air cooled. Afterwards they were recrystallized at 780°C for 2 h and water quenched.

Then all specimens were held at ageing temperatures of 550°C, 600°C, 650°C, 700°C and 750°C for different periods of time, to establish the equilibrium concentration of antimony at the grain boundaries. The time necessary for equilibration at each temperature can be assessed using an equation proposed by McLean[6]. AES measurements confirmed that the calculated time was long enough to reach equilibrium segregation; the conditions of each exposure are listed in **Table 2**.

Table 2: Conditions for the establishment of segregation equilibria

Ageing Temperature/ Ageing Time	Exposure Conditions
550°C/600 h	vacuum/quenched in water
600°C/140 h	vacuum/quenched in water
650°C/ 50 h	flowing argon/quenched in water
700°C/ 5 h	flowing argon/quenched in water
750°C/ 2 h	flowing argon/quenched in water

The amount of grain boundary segregation was to be measured by AES, which is conducted in UHV to avoid surface contamination. After cooling to about -120°C the cylindrical notched specimens were fractured by impact in the UHV chamber of the spectrometer. The fracture surface was then imaged by operating the electron beam in a scanning electron microscope (SEM) mode to distinguish between intergranular and transgranular areas. Auger spectra were taken from at least 10 individual grain boundary facets using a cylindrical mirror analyzer (CMA) and the results were averaged. The peak-to-peak heights of antimony (454 eV), nickel (848 eV) and carbon (271 eV) were related to the iron peak at 651 eV. The entire analysis of each fracture face had to be completed within approximately 3 h to prevent contamination effects. The operating conditions were as follows: primary beam energy 5 kV, primary beam current 3 x 10^{-6} A, and primary beam size 10 µm.

To estimate the degree of coverage of antimony at the grain boundaries, it can be assumed that antimony is uniformly distributed on both fracture faces. This supposition was verified by some AES measurements in which opposite fracture facets were investigated[7]. From LEED studies of surface segregation on Fe-Sb single crystals a calibration factor had been obtained which converts the peak-to-peak height ratio to the degree of coverage[8].

Supplementary surface analytical methods were employed. The binding state of core electrons of segregated antimony was determined by X-ray photoelectron spectroscopy (XPS), while scanning Auger microscopy (SAM) was applied to examine the distribution of segregated elements on grain boundary facets.

The fracture type and the mechanical properties were investigated using SEM (accelerating voltage 20 kV) and Charpy impact tests (DIN 50115).

3 Results and discussion

3.1 Fe-Sb alloys

Typical Auger spectra of transgranular and intergranular areas are represented in **Figure 1**. On transgranular fracture surfaces of the Fe-0,094 wt.% Sb alloy, no antimony peak was observed, since the bulk concentration is below the detection limit of the AES method. The oxygen peak is due to adsorption from the residual atmosphere after breaking the sample. The spectrum taken on a grain surface of the same alloy clearly indicates the enrichment of antimony which is caused by grain boundary segregation.

Figure 2 illustrates that the average coverage of antimony at the grain boundaries increases with increasing bulk concentration and decreasing equilibration temperature. The scatter of the data indicated by the error bars in one curve is rather large (25% - 30% of the mean value) due mainly to the following reasons:

a) The segregation of antimony may be strongly dependent on grain orientation as indicated by surface segregation studies on Fe-Sb single crystals[8].

b) The examined areas have different distances and different surface normals to the cylindrical mirror analyzer (CMA).

c) The degree of coverage is calculated from measurements on only one side of the intergranular fracture face. It was verified by some AES measurements in which opposite fracture facets were investigated that the average grain boundary antimony concentration is nearly the same on both fracture faces[7]. The assumption that an-

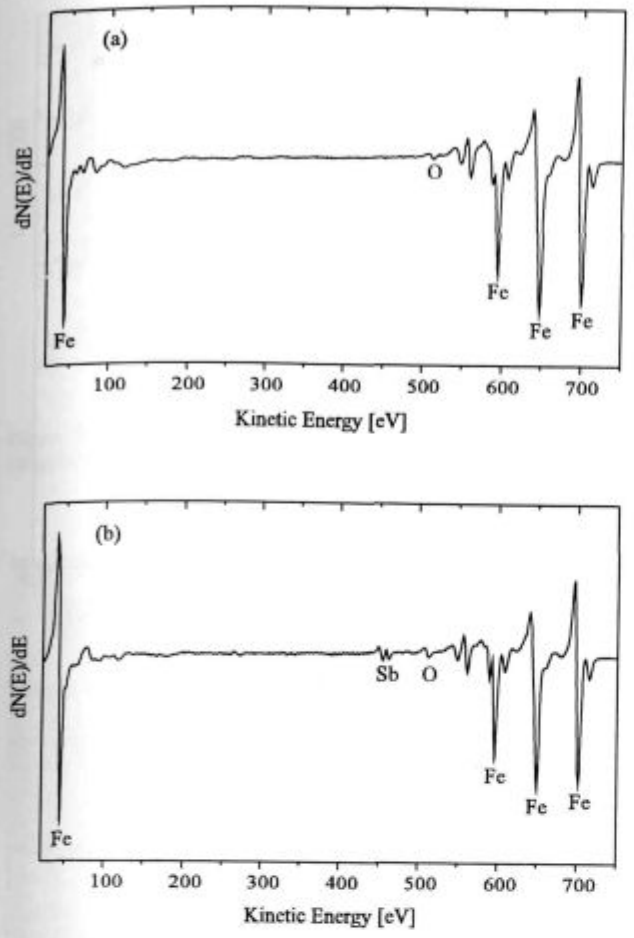

Figure 1: Auger spectra of fracture surfaces of Fe - 0,094 wt.% Sb alloy after annealing at 650°C. a) cleavage facet, b) intergranular fracture surface

Slika 1: AES spekter prelomnih površin Fe - 0,094 ut.% Sb po žarjenju pri 650°C. a) prelomna ploskev, b) interkristalna prrlomna površina

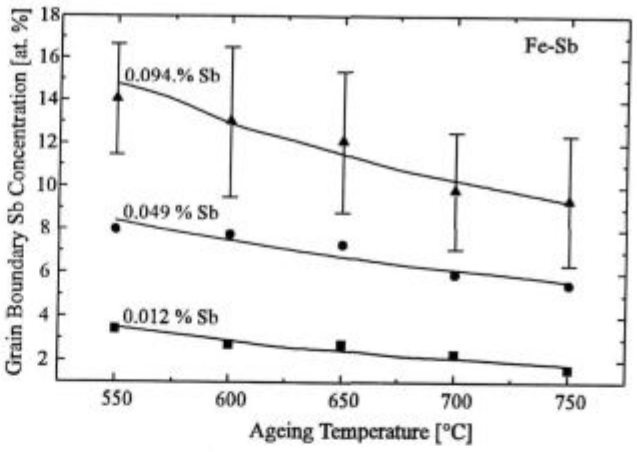

Figure 2: Grain boundary concentration of antimony plotted as a function of equilibration temperature for the alloys Fe - 0,012 wt.% Sb, Fe - 0,049 wt.% Sb and Fe - 0,094 wt.% Sb

Slika 2: Koncentracija antimona na kristalni meji kot funkcija ravnotežne temperature za zlitine Fe - 0,012 ut.% Sb, Fe - 0,049 ut.% Sb in Fe - 0,094 ut.% Sb

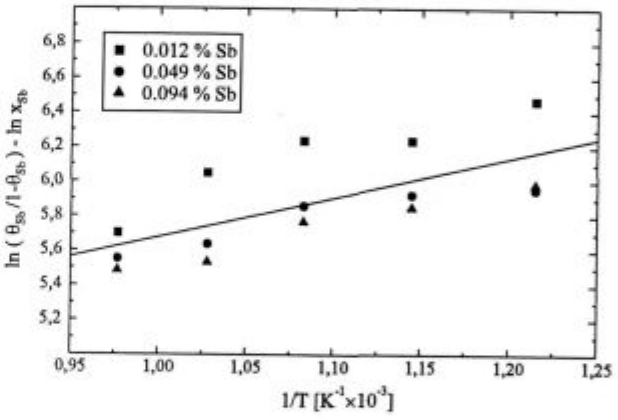

Figure 3: Langmuir-McLean plot of the data in **Figure 2**

Slika 3: Langmuir-McLeanov diagram podatkov iz **slike 2**

timony is equally distributed is probably not true for each single intergranular area.

In spite of the large scatter of the data, a thermodynamic calculation was attempted, applying the Langmuir-McLean equation

$$\ln\frac{\theta}{1-\theta} - \ln x_{Sb} = -\frac{\Delta H_{segr}}{RT} + \frac{\Delta S^{exs}_{segr}}{R} \qquad (1)$$

which expresses the relationships between bulk concentration (mole fraction) x_{Sb}, temperature T, and degree of coverage θ, at the grain boundaries. The results according to the Langmuir-McLean equation are plotted in **Figure 3**. The estimation yields the segregation enthalpy $\Delta H_{segr.}$ = -19 kJ/mol ± 5 kJ/mol and the segregation entropy $\Delta S_{segr.}$ = 28 J/mol K ± 6 J/mol K. The free enthalpy of segregation in α-iron can be expressed as follows:

$$\Delta G_{segr} = -(19\ \text{kJ/mol} \pm 5\ \text{kJ/mol}) - T(28\ \text{J/mol K} \pm 6\ \text{J/mol K})$$

The segregation enthalpy value is low compared to values for phosphorus (ΔH_{segr} = -34 kJ/mol)[9] or tin (ΔH_{segr} = -23 kJ/mol)[10], this indicates the low tendency for grain boundary segregation of antimony in iron.

It would be unreasonable in the present thermodynamic calculations to include the AES data for the Fe - 0,93 wt.% Sb and Fe - 1,91 wt.% Sb alloys, since unknown antimonides had formed at the grain boundaries. In **Figure 4**, a typical scanning electron micrograph and the corresponding elemental map for antimony on the same intergranular area of the Fe - 0,93 wt.% Sb alloy indicate star shaped antimonides.

In spite of the low tendency for grain boundary segregation, antimony has a strongly embrittling effect. The relationship between the percentage of intergranular fracture and the grain boundary coverage of antimony is demonstrated in **Figure 5**. With increasing enrichment of antimony at the grain boundaries the fracture mode at

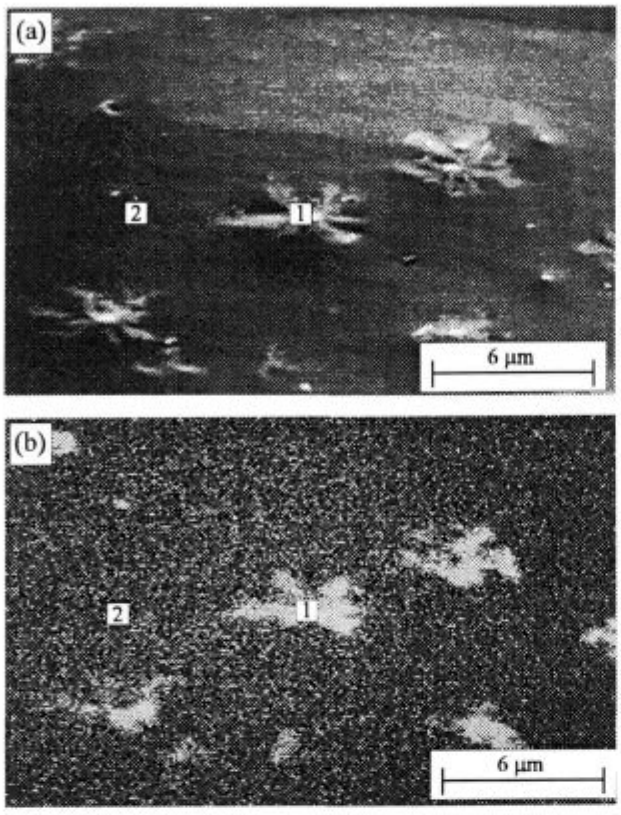

Figure 4: Intergranular antimonides observed in Fe - 0,93 wt.% Sb after annealing at 650°C; a) scanning electron micrograph, b) corresponding scanning Auger image of Sb

Slika 4: Interkristalni antimonidi opaženi v Fe - 0,93 ut.% Sb po žarjenju na 650°C; a) posnetek z vrstičnim elektronskim mikroanalizatorjem, b) vrstični Augerjev posnetek

low temperatures (about -120°C) changes from transgranular to intergranular already at rather low grain boundary concentrations.

The influence of antimony segregation on the mechanical properties was also studied by Charpy impact testing. The transition temperature determined T_T is a measure of the embrittlement of iron base alloys. T_T is defined as the temperature where half of the difference value between the impact work necessary for ductile fracture and the impact work for brittle fracture is reached. For the Fe-Sb alloys a shift of the impact transition temperature to higher values is expected with increasing antimony concentration at the grain boundaries. This supposition is verified in **Figure 6**. For each of the two investigated alloys a higher transition temperature is obtained with increasing coverage of antimony at the grain boundaries. However, the Fe - 0,094 wt.% Sb alloy tempered at 750°C has a lower transition temperature than the Fe - 0,049 wt.% Sb alloy annealed at the same temperature. The observed phenomenon can be explained by the different average grain size of these materials (Fe - 0,049% Sb: 0,21 mm; Fe - 0,094% Sb: 0,08 mm), with increasing antimony concentration the grain

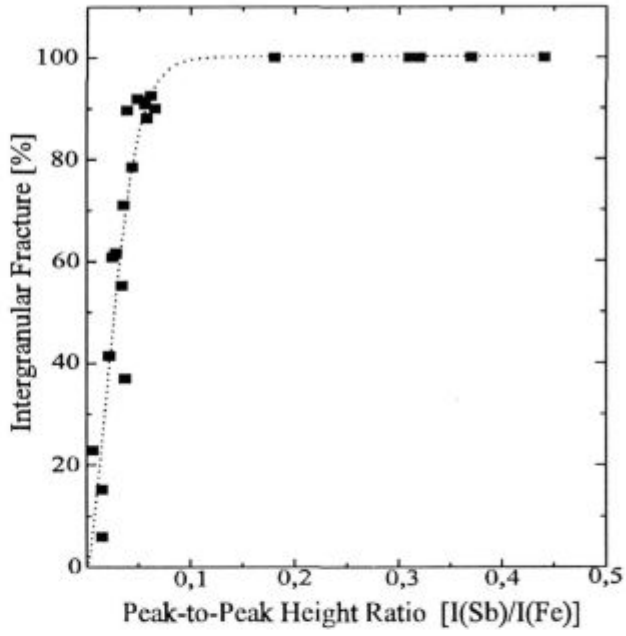

Figure 5: Percentage of intergranular fracture versus peak-to-peak height ratio I(Sb)/I(Fe)

Slika 5: Odstotek interkristalnega preloma v odvisnosti od razmerja višine vrhov I(Sb)/I(Fe)

size decrease which leads to a higher strength of the material.

One possible way to explain the embrittling behaviour of antimoy is to apply quantum mechanical models[11,12]. The main conclusions of these calculations can be summarized as follows:

The segregated antimony atoms are electronegative with respect to the host metal iron. Consequently electronic charge is transferred from iron to antimony. This charge transfer leaves fewer electrons to participate in

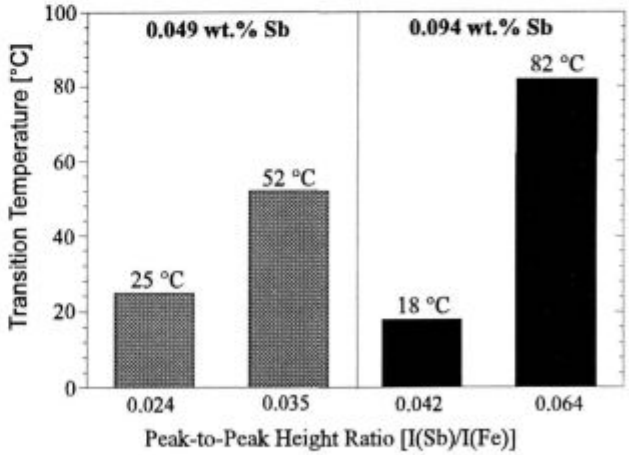

Figure 6: Dependence of the transition temperature on the grain boundary antimony concentration for Fe - 0,049 wt.% Sb and Fe - 0,094 wt.% Sb alloys

Slika 6: Odvisnost koncentracije antimona na mejah zrn od prehodne temperature za zlitine Fe - 0,049 ut.% Sb in Fe - 0,094 ut.% Sb

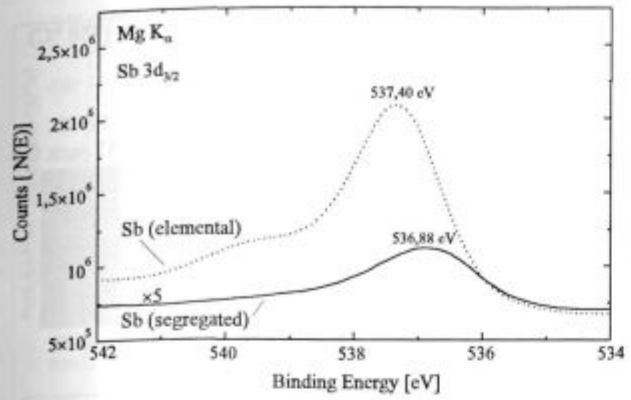

Figure 7: Photolines of pure Sb and segregated Sb in Fe-Sb alloys
Slika 7: XPS krivulje čistega Sb in segregiranega Sb v Fe-Sb zlitini

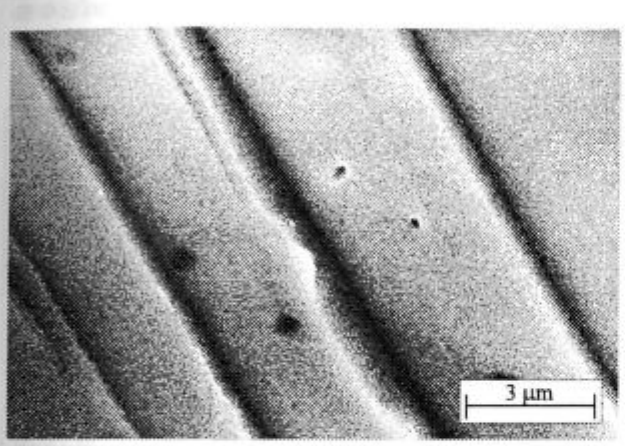

Figure 8: SEM of a faceted grain boundary in Fe - 0,094 wt.% Sb after annealing at 650°C
Slika 8: SEM posnetek facetirane meje v zlitini Fe - 0,094 ut.% po žarjenju na temperaturi 650°C

the iron-iron bonding and these bonds at the grain boundary will be weakened.

XPS measurements on a large area of intergranular fracture of Fe - 0,93 wt.% Sb alloy after annealing at 600°C show that the energies of the Sb 3d electron levels of segregated and pure antimony are distinctly different (**Figure 7**). The energy shift of about -0,5 eV in comparision to pure antimony indicates an electron transfer to segregated antimony, as expected in the above model.

It is also possible to explain the embrittling behaviour of antimony in another way by taking into consideration that the grain boundaries often are facetted, as illustrated in **Figure 8**. The segregation of antimony induces a reconstruction of the grain faces which results in a decrease of grain boundary cohesion.

On some intergranular areas pores were detected with an average diameter of 2 µm as can be seen in **Figure 9**. An antimony map recorded for the same area, shows antimony enrichment within this pore. Segregated antimony certainly favours the formation of such pores since its surface segregation causes a pronounced decrease of

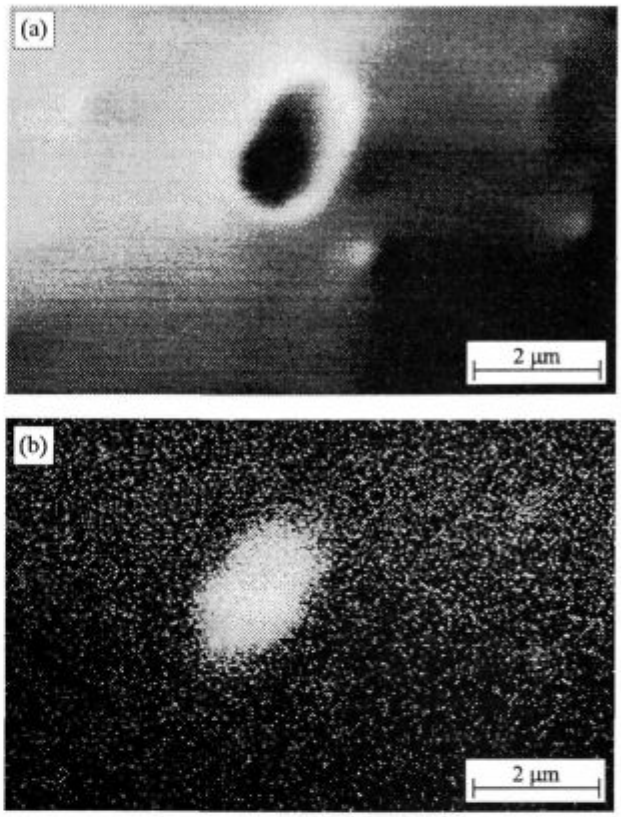

Figure 9: Pore at a grain boundary facet of Fe - 0,094 wt.% Sb after annealing at 600°C; a) SEM, b) corresponding scanning Auger image of Sb
Slika 9: Razpoka v kristalni meji Fe - 0,094 ut.% po žarjenju na temperaturi 600°C; a) SEM posnetek, b) odgovarjajoči SAM posnetek Sb

surface energy and such pores will intensity the observed embrittlement of the material.

3.2 Fe-C-Sb alloys

Samples with different antimony and carbon contents were investigated to study the effect of carbon on antimony grain boundary segregation. The fracture faces of the Fe-C-Sb alloys with 0,049 wt.% Sb show transgranular fracture caused by the carbon content. The higher cohesion of these materials compared with corresponding Fe-Sb alloys is due to the fact that antimony is displaced from the grain boundaries by carbon, according to the equation

$$\text{C(dissolved)} + \text{Sb(segregated)} = \text{C(segregated)} + \text{Sb(dissolved)} \qquad (2)$$

The mutual displacement of these two elements corresponding to the displacement equilibria in the systems Fe-C-P[9] and Fe-C-Sn[10], was proven for the Fe-C-Sb alloy with 0,094 wt.% Sb, as shown in **Figure 10**. The average grain boundary concentration of antimony decreases with increasing grain boundary and bulk concentration of carbon. Simultaneously the percentage

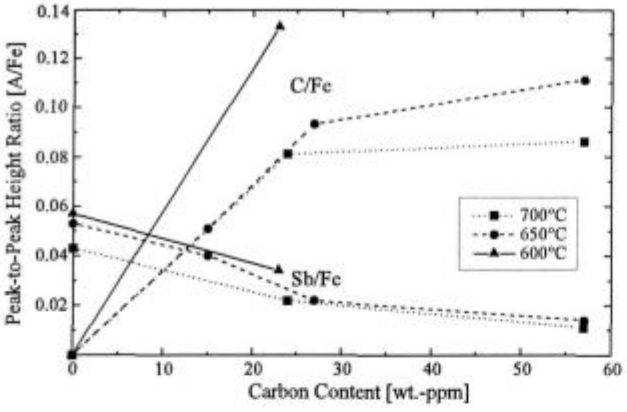

Figure 10: Dependence of the Sb and C grain boundary concentrations on the bulk concentration of carbon in Fe - 0,094 wt.% Sb

Slika 10: Odvisnost koncentracij Sb in C na mejah zrn od koncentracije ogljika v osnovnem materialu Fe - 0,094 ut.% Sb

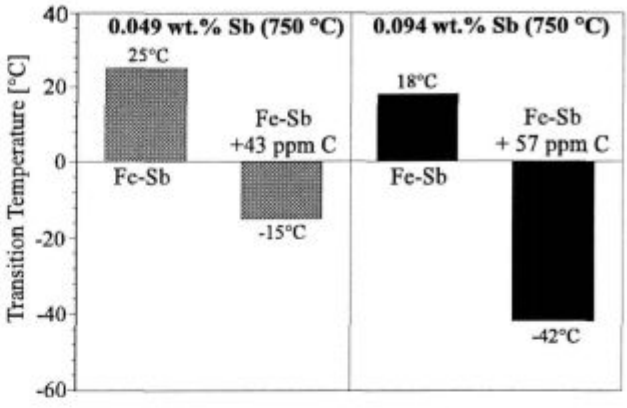

Figure 12: Dependence of the transition temperature on bulk concentration of carbon for Fe - 0,040 wt.% Sb and Fe - 0,094 wt.% Sb after annealing at 750°C

Slika 12: Odvisnost prehodne temperature žilavosti od vsebnosti ogljika v osnovnem materialu Fe - 0,049 ut.% Sb in Fe - 0,094 ut.% Sb po žarjenju na temperaturi 750°C

of transgranular fracture rises with increasing bulk concentration of carbon (**Figure 11**).

The decrease of brittle intergranular fracture of Fe-C-Sb alloys can be explained by the following effects:

a) The strongly embrittling antimony is displaced from the grain boundaries by carbon.

b) The segregated carbon causes a higher grain boundary cohesion.

If energetic interactions between segregated carbon and antimony are neglected, the above mentioned phenomena can be described by considering only the site competition of the two elements

$$\frac{\theta_{Sb}}{1-\theta_{Sb}-\theta_C} = x_{Sb} \exp\left(\frac{-\Delta G^0_{Sb}}{RT}\right) \quad (3)$$

$$\frac{\theta_C}{1-\theta_{Sb}-\theta_C} = x_C \exp\left(\frac{-\Delta G^0_C}{RT}\right) \quad (4)$$

The de-embrittling effect of carbon was also demonstrated by Charpy impact tests. **Figure 12** illustrates for

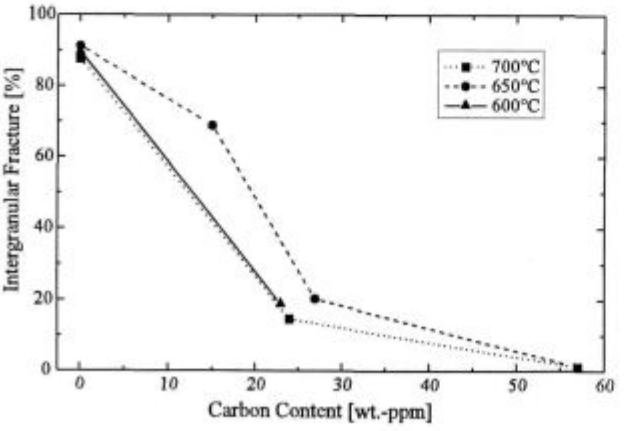

Figure 11: Variation of the percentage of intergranular fracture with bulk concentration of carbon in Fe - 0,094 wt.% Sb

Slika 11: Sprememba odstotka interkristalnih prelomnih ploskev v odvisnosti od koncentracije ogljika v zlitini Fe - 0,094 ut.% Sb

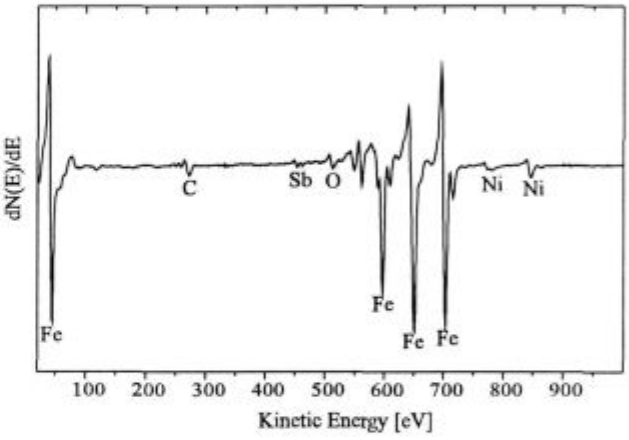

Figure 13: Auger spectrum of an intergranular fracture surface of Fe - 2,85 wt.% Ni - 0,049 wt.% Sb

Slika 13: AES spekter interkristalne prelomne površine zlitine Fe - 2,85 ut.% Sb

both Fe-Sb alloys (0,049 wt.% Sb or 0,094 wt.% Sb) tempered at 750°C that the transition temperature shifts to lower values if carbon is added to each alloy.

3.3 Fe-Ni-Sb alloys

The influence of nickel on the grain boundary segregation of antimony was also investigated for two Fe-Ni-Sb alloys. Auger spectra taken from intergranular areas indicate the enrichment of antimony and nickel; a typical Auger spectrum is shown in **Figure 13**. The temperature dependence of antimony and nickel equilibrium segregation contradicts previous results of other authors[2,4,5] (**Figure 14**). No evidence was found for cosegregation of antimony and nickel or for antimony segregation beeing enhanced by the presence of nickel, as was observed by other authors[2,4]. For the Fe - 0,53 wt.% Ni - 0,049 wt.% Sb alloy the antimony grain boundary concentration is

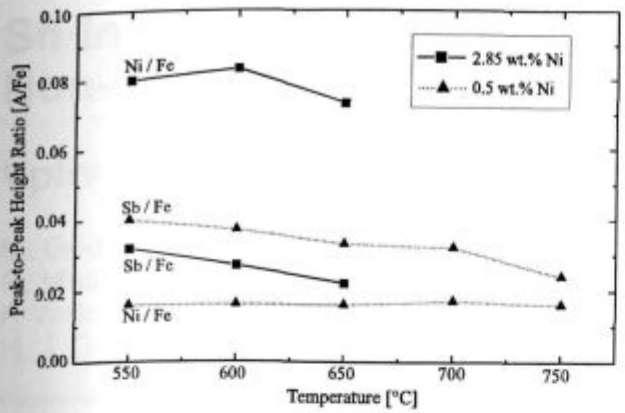

Figure 14: Grain boundary segregation of Sb and Ni plotted as a function of equilibration temperature for two Fe-Ni-Sb alloys
Slika 14: Segregacija Sb in Ni po mejah zrn prikazana kot funkcija ravnotežne temperature za dve zlitini Fe-Ni-Sb

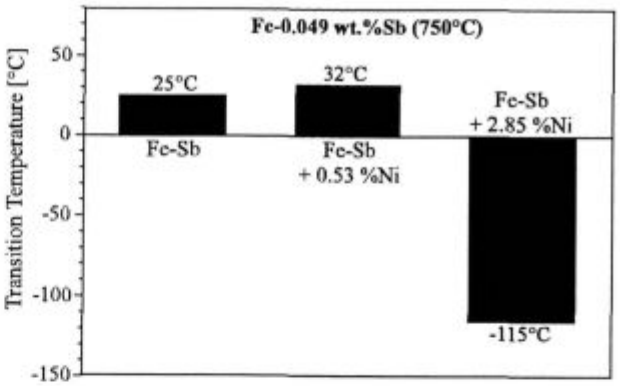

Figure 15: Dependence of the transition temperature on the bulk concentration of nickel for Fe-Ni- 0,049 wt.% Sb alloys after annealing at 750°C
Slika 15: Odvisnost prehodne temperature žilavosti od vsebnosti niklja v Fe-Ni- 0,049 ut.% Sb po žarjenju na 750°C

nearly the same at all temperatures as for the same alloy without nickel and is therefore not enhanced by the presence of nickel. Additionally, the amount of nickel segregation is always the same at all temperatures. AES studies on the Fe - 2,85 wt.% Ni - 0,049 wt.% Sb alloy illustrate that the average amount of antimony is lower than in the Fe - 0,53 wt.% Ni - 0,049 wt.% Sb alloy. The grain boundary concentration of antimony increases with decreasing annealing temperature, but the behaviour of nickel is slightly different. After increasing segregation with decreasing temperature the grain boundary segregation of nickel decreases at 600°C. Consequently Guttmann's model of cosegregation does not hold true for the Fe-Ni-Sb system. It was also asserted that the presence of nickel enhances the embrittling behaviour of antimony. Charpy impact tests of Fe-Ni-Sb alloys tempered at 750°C show different results (**Figure 15**). The transition temperature of Fe - 0,049 wt.% Sb and Fe - 0,53 wt.% Ni - 0,049 wt.% Sb alloy is nearly the same, while the transition temperature of Fe - 2,85 wt.% Ni - 0,049 wt.% Sb alloy decreases to a value which is typical for ductile materials. With regard to this result the deembrittling effect of nickel can be explained by the following effects:

a) Nickel promotes the refinement of grains.

b) The segregation decrease in antimony may be due to nickel segregation.

Thus the expected severe embrittlement of Fe-Ni-Sb alloys according to earlier investigations was not confirmed.

4 Acknowledgement

The authors are grateful to the European Committee for financial support under contract no. P3455.

5 References

[1] J. Kameda, C. J. McMahon, *Met. Trans. A*, 12A, 1981, 31
[2] C. L. Briant, A. M. Ritter, *Acta Met.*, 32, 1984, 11, 2031
[3] C. L. Briant, H. J. Grabke, *Materials Science Forum*, 46, 1989, 260
[4] P. Gas, M. Guttmann, J. Bernardini, *Acta Met.*, 30, 1982, 1309
[5] A. Wirth, I. Andreoni, G. Gregory, *Surface and Interface Analysis*, 9, 1986, 157
[6] D. McLean, Grain Boundaries in Metals, Oxford University Press., Oxford, 19577, 131
[7] H. Viefhaus, R. Mast, unpublished results
[8] M. Rüsenberg, H. Viefhaus, *Surface Science*, 172, 1986, 615
[9] H. Erhart, H. J. Grabke, *Metal Science*, 15, 1981, 401
[10] W. Jäger, H. J. Grabke, Jin Yu, *Proc. Int. Conf. on 'Residuals and Trace Elements in Iron and Steel*, Portorož, Oct. 1985, ed. by F. Vodopivec, Inst. Metall., Ljubljana, 1986, 217-237
[11] C. L. Briant, R. P. Messmer, *Acta Met.*, 32, 1984, 11, 2043
[12] W. Losch, *Acta Met.*, 27, 1979, 1885